Analysis of Measured and Theoretically Predicted Temperature Field in High-Temperature Asphalt Pavement during Daily Cycle

Zhonghai Jiang[1], Qian Wang[1], Liangbing Zhou[2]*

[1] School of Transportation and Civil Architecture, Foshan University, Foshan, Guangdong, China

[2] Guangdong Yuanshun Architectural Design Co., Ltd., Foshan, Guangdong, China

*Corresponding Author.

Abstract:

To accurately predict the temperature field in high-temperature asphalt pavement, this paper analyzed the daily variations in the temperature field within high-temperature asphalt pavement. Both the variation law of air temperature and solar radiation intensity were fitted with a double sine function and quasi-normal distribution function. Furthermore, an empirical prediction model was constructed to determine the pavement's surface temperature. To carry out theoretical predictions and as the boundary conditions of the temperature field, the asphalt pavement was simplified into a single-layer or a double-layer flat plate structure. Based on the obtained results, the predictions of the model with an exact solution for the temperature field was analyzed. The maximum daily average absolute deviation between the predicted and measured data amounted to 1.24 °C. These results indicate a high prediction accuracy.

Keywords: High Temperature, Asphalt pavement, Temperature field, Prediction.

I. INTRODUCTION

The surface temperature of asphalt pavement exposed to the external environment constantly varies due to environmental factors such as air temperature and solar radiation. This generates an unstable heat conduction within the asphalt pavement and results in a non-uniform and unstable distribution of the temperature field along depending on depth. Furthermore, as the asphalt mixture is sensitive to temperature variation, asphalt pavement performance is easily damaged by a change in the temperature field. In long-term high-temperature environments, the strength and stiffness of the pavement will decrease under repeated loading. This will, in turn, result in insufficient resistance and lead to permanent deformation, typically represented by rutting of the pavement [1, 2].

In 2011, Rongbin et al. [3] proposed a modified one-dimensional heat transfer model. By creating a meteorological database and optimizing pavement parameters for a specific location, the model was able to

calculate hourly pavement temperatures, with the results being in agreement with the measured values. In 2013, Mostafa A. Abo-Hashema [4] tested actual pavement temperatures and established two neural network models for predicting temperature within the asphalt concrete layer. The first model was based on air temperature as well as other parameters and accounted for cases when parameters were unavailable, while the second model was based solely on air temperature. To accurately calculate the viscoelastic response of asphalt concrete pavements under traffic and thermal loads, Mohammad Z. Alavi et al. [5] proposed a fully implicit temperature field prediction method based on the finite control volume method in 2014. In 2015, Ariawan I M A et al. [6] continuously collected data for variations in air temperature, air humidity, and the pavement temperature at different depths of the western national road on Bali, Indonesia. Furthermore, by taking air temperature and air humidity as independent variables, the researchers established a linear regression model for predicting asphalt pavement temperature. To evaluate the urban climate formed in the built environment, Shashwath Sreedhar et al. [7] constructed a pavement temperature prediction model based on the thermophysical properties of different pavements. The pavement types included cement concrete pavement, conventional and modified asphalt pavement. The model required the thermophysical parameters of different pavement materials, including the specific heat capacity, thermal conductivity, material density, air temperature, wind speed, and air relative humidity. Furthermore, Anush K. Chandrappa et al. [8] established a pavement temperature model based on meteorological factors and verified it in combination with the US long-term pavement performance (LTPP) climate database. Lastly, in 2017, Amani Al-Kalbani et al. [9] constructed a model for measuring asphalt pavement temperatures. The model was based on the relationship between air temperature and pavement temperature and was used to predict temperatures in asphalt pavement in Muscat, Oman.

At present, a number of studies have predicted the temperature field in asphalt pavement through statistical analysis. However, these studies considered solely the effects of external factors and neglected the characteristics of pavement structure itself. This type of oversight has resulted in models with an insufficient prediction accuracy which are suitable only for local areas. The present study establishes an empirical prediction model for the surface temperature of asphalt pavement. The model clarifies the relationship between the external environment and temperature field within asphalt pavement. In turn, this relationship functions as the boundary conditions for establishing a theoretical prediction model with higher prediction accuracy.

II. TESTS AND METHODS

2.1 Collecting Data of the Temperature Field

This study measured the temperatures at different depths in the asphalt pavement and collected external meteorological data. To generalize the measured data, an open field with few obstacles was selected as the monitoring site. Fig 1 illustrates the test pavement's structure and the arrangement of the temperature sensors:
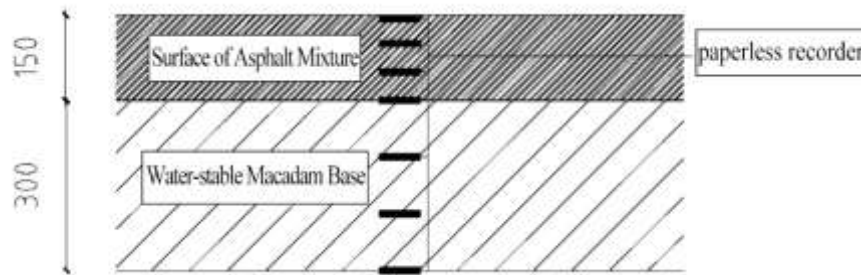
Fig 1: Temperature collection in asphalt pavement (thickness: mm)

The pavement temperatures were collected by temperature sensors and a paperless recorder. The temperature sensors were made of stainless steel (Pt100, Songdao, as shown in Fig 2), equipped with nut and high-temperature sealing rings, which were waterproof, resistant to high-temperature and high-pressure. Their measuring range was between -50~420 °C, while their precision was 0.1 °C. Before being embedded, all the sensors were calibrated with the same mercury thermometer. To prevent possible damage, two sensors were embedded at each temperature measurement point. A ten-channel universal paperless recorder was used to record the collected temperature signal every 10 min, as shown in Fig 3.

Fig 2: Pt100 temperature sensor   Fig 3: Multi-channel paperless recorder

The meteorological data necessary for the test was solar radiation intensity, air temperature, relative humidity, and wind speed. Furthermore, an outdoor climate environment test system (JTR13, Beijing Century Jiantong, China, as shown in Fig 4) collected this data regularly, with the collection precision being 1 W/m2, 0.1 °C, 1% and 0.1 m/s, respectively. Lastly, the acquisition interval was set to 10 min.

Fig 4: JTR13 Outdoor climate environment test system

The monitoring test was conducted in September 2020. The weather conditions were such that there was no rain, and the temperature was higher than 55 ℃. Data with a day cycle was collected continuously for 24 hours.

2.2 Distribution Law of the Temperature Field in High-Temperature Asphalt Pavement

Asphalt pavements are continuously affected by external meteorological environmental factors. Therefore, the temperature distribution inside the structure experiences periodic variation. Furthermore, due to the heat conduction process inside the pavement, the temperatures at different depths are differently sensitive to variations in the external environment [10, 11]. Based on the measured pavement's temperature field in high-temperature weather, this section analyzes daily temperature variation at different depths within the pavement, as well as the temperature distribution in the asphalt pavement at different times of the day.

External environmental factors affecting the temperature field, such as the air temperature and solar radiation vary periodically during a 24-hour period. Therefore, their impacts on the temperature field within asphalt pavement also vary periodically within a 24-hour period [12, 13]. Fig 5 illustrates the daily temperature variations at different pavement depths on September 5th, 2020, which was taken as the representative day.
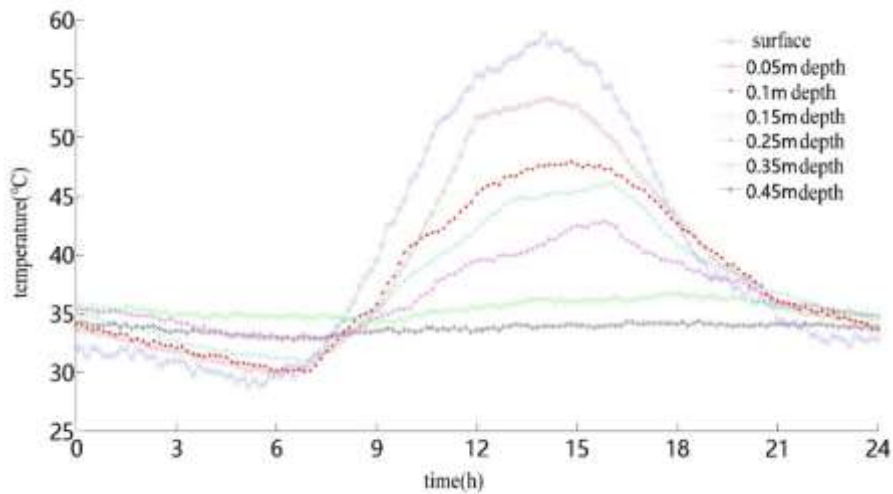
Fig 5: Daily variation in temperature at different pavement depths

Several conclusions may be drawn by Fig 5:

(1) The asphalt pavement temperature exhibits an initially decreasing trend, followed by an increase and a final decrease during the whole day. In general, the pavement temperature rises from 6:00 am to 15:00 pm, when it begins to decrease due to a continuous decrease in both solar radiation intensity and temperature.

(2) Secondly, during the entire day, the maximum and minimum pavement temperatures appear on the surface level. The daily minimum surface temperature appears around 6:00 am, while the daily maximum occurs at around 2:30 pm. Furthermore, as the pavement depth increases, the temperature fluctuation gradually begins to lag. For instance, compared to the time when the surface layer reaches its maximum, the time for the interface of the surface layer and base layer lags by about 2 hours.

(3) Lastly, the surface temperature exhibits the largest daily variation. The largest daily difference in the surface temperature is 29 °C. Conversely, with the increase in pavement depth, the daily temperature variation gradually decreases. Furthermore, the sensitivity to variations in the external environment gradually decreases as well. Consequentially, the bottom temperature of the pavement's base layer exhibits the smallest daily variation. Fig 5 illustrates the daily variation in temperature being only 2 °C, while the temperature variation curve is relatively smooth. Thus, in the following theoretical and numerical calculation of the asphalt pavement's temperature field, the bottom temperature of the base layer is considered to be constant.

The difference in the thermophysical properties of the surface layer and base material, alongside the variation in external environmental conditions all lead to a non-uniform and unstable distribution of pavement temperature at varying depths. The temperature distributions at different pavement depths and at different times on September 5th, 2020, are as Fig 6~Fig 8:
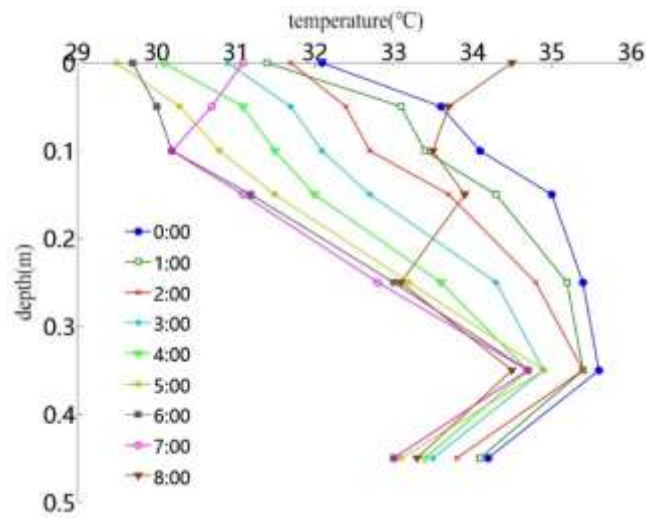
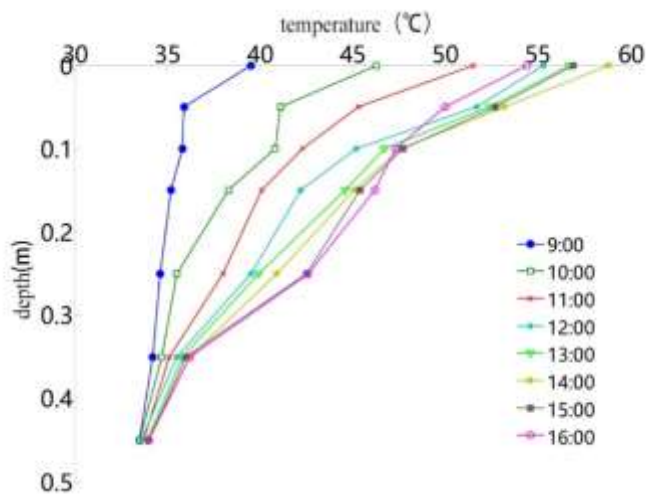Fig 6: Temperature distribution from midnight to 8 a.m.

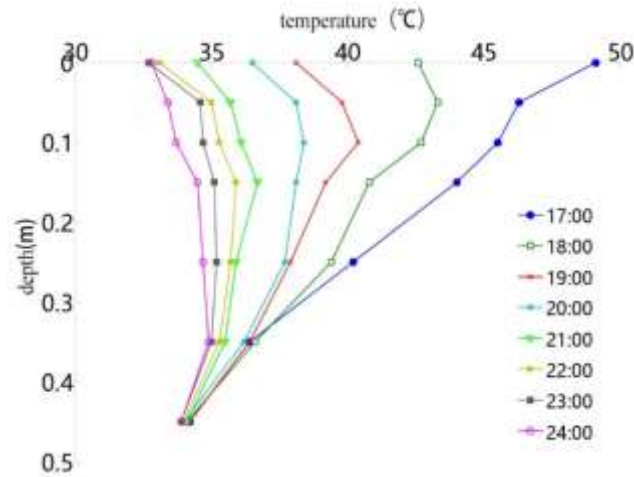Fig 7: Temperature distribution from 9:00 a.m. to 04:00 p.m.

Fig 8: Temperature distribution from 5 p.m. to midnight

The following conclusions may be drawn from the data presented in Fig 6, Fig 7, Fig 8:

(1) In relation to depth, the pavement temperature exhibits a nonlinear variation. The overall temperature gradient of the surface layer is large, with the maximum daily difference between the surface and bottom surface layer reaching 17 °C. Furthermore, the overall temperature gradient of the base layer was observed to be relatively small. More specifically, the maximum daily temperature difference was only 12 °C even though the thickness of the base layer is twice that of surface layer.

(2) Secondly, from around 6:00 a.m., the pavement temperature exhibited a downward trend. In other words, as the depth increased, the temperature gradually increased. Furthermore, due to temperature increase and higher solar radiation intensity, the pavement temperature gradually increased from 6:00 a.m. to 02:00 p.m. The surface layer exhibits the fastest temperature rise. On the other hand, the deeper the layer, the later the start time of the rise in temperature. With the decrease in air temperature and solar radiation that occurs after 3:00 p.m., the pavement's temperature also gradually decreases away from the surface. Due to faster heat dissipation, and especially the lack of solar radiation after sunset, the shallower surface layers experience a significant drop in temperature. Lastly, the above figures show that pavement temperature initially increases and decreases with the increase in depth.

2.3 Empirical Prediction Model for Surface Temperature

When the asphalt pavement is directly exposed to the natural environment, it is affected by a number of environmental factors. Furthermore, because the surface layer is in direct contact with the external environment, it is most affected by it and its variations [14, 15]. The fluctuation in surface temperature is related to external environmental factors and may affect variations within the temperature field as the upper boundary condition of the heat conduction process inside the pavement. Therefore, understanding the relationship between road surface temperatures and environmental factors is essential for calculating and predicting pavements' temperature fields [16, 17].

There are three ways of transferring heat between asphalt pavement and the external environment: convective heat transfer, solar radiation, and effective pavement radiation. Of the three, solar radiation may be directly measured. Conversely, determining convective heat transfer and effective pavement radiation involves parameters that are difficult to determine. In general, these parameters are empirically determined within a rough range, which makes it difficult to establish the relationship between the pavement's temperature field and the external environment. Because of this, the current paper uses an analysis method to establish an empirical prediction model for asphalt surface temperature. This model is based on the three main meteorological factors: air temperature, wind speed, and solar radiation intensity [18, 19].

Previous studies claim that air temperature and solar radiation have the greatest impact on the temperature field in high-temperature asphalt pavement. A comparison between the measured temperature, surface temperature, and solar radiation intensity on September 5th, 2020, is illustrated in Fig 9.
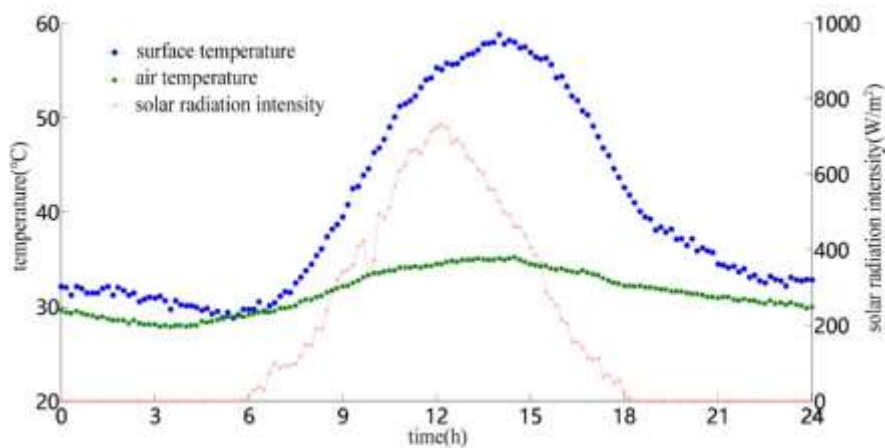

Fig 9: Daily variations in surface temperature, air temperature, and solar radiation intensity

The variations in surface temperature and air temperature are similar within a 24-hour period. Here, the highest daily surface temperature and highest daily air temperature both occur between 02.00 p.m. 03.00 p.m. Furthermore, solar radiation intensity peaks around 12:00 a.m., about two and a half hours earlier than when the maximum surface temperature was measured.

Because a single sine function is unable to accurately represent the daily temperature variations, this paper employs a model composed of two sine functions. The model is represented in Equation (1):

$$T_a(t) = \bar{T}_a + T_m[A\sin\omega(t - C) + B\sin2\omega(t - C)] \qquad (1)$$

In the above Equation, $\bar{T}_a$ represents the average value of the daily maximum and minimum temperatures. Furthermore, T_m denotes the daily temperature amplitude, while $\omega = \pi/12$ and A, B, and C denote fitting parameters, whose precision is measured to 0.01. The fitting results are provided in

8

TABLE I.

TABLE I. Fitting results of the parameters of the daily temperature variation model

PARAMETER/DATE	A	B	C
September 5th	0.86	0.20	8.38
September 11th	0.85	0.19	8.42
September 13th	0.86	0.17	8.41

In general, it is difficult to obtain prediction data for solar radiation directly from weather stations. Daily variations of solar radiation follow a normal distribution pattern, while the magnitude of the solar radiation intensity positively correlates with the daily maximum temperature in high-temperature and sunny weather. Therefore, the present paper used Equation (2) to predict the daily variations in the solar radiation intensity.

$$Q(t) = A'T_{amax}e^{-\frac{(t-B')^2}{C'^2}} \tag{2}$$

In the above Equation, T_{amax} represents the daily maximum temperature, which may be obtained directly from weather station. Furthermore, A', B' and C' denote fitting parameters, whose precision is 0.1. The fitting results are provided in TABLE II.

TABLE II. Fitting results of the model parameters for the daily variations in solar radiation intensity

PARAMETER/DATE	A	B	C
September 5th	19.8	12.2	3.7
September 11th	19.5	12.4	3.5
September 13th	19.8	12.0	3.5

The advantage of the models represented by Equation 1 and Equation 2 is that the daily variation curve can be obtained using only the daily maximum and minimum temperatures, which are easier to obtain in practical prediction and applications. The necessary parameters were obtained by taking the average value of fitting the short-term measured data. Thus, it is necessary to re-fit and re-determine parameters for different latitude regions and for different seasonal climates.

The temperature and solar radiation intensity were measured for September 5th, while predictions were made according to Equation 1 and Equation 2 with only the daily maximum and minimum temperatures being provided. The comparison results with the measured values are as Fig 10, Fig 11.
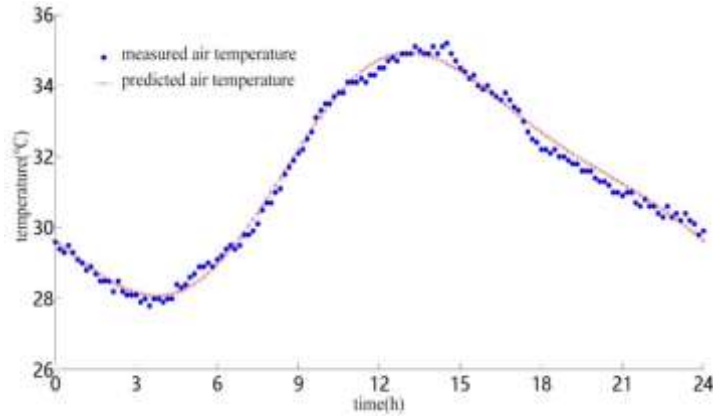
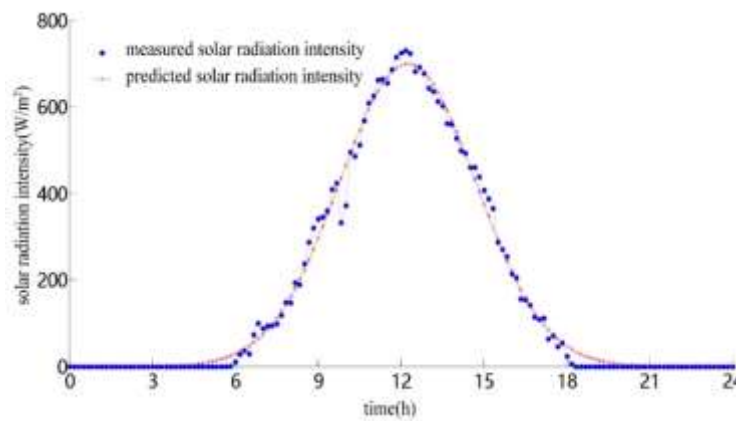Fig 10: Comparison of measured and predicted air temperature

Fig 11: Comparison of measured and predicted solar radiation intensity

The predicted temperatures and solar radiation intensity appear to be in agreement with the measured values. The average prediction errors are 0.18 °C and 12 W/m^2, with the correlation coefficients being 0.986 and 0.981, respectively. These results indicate that models used for predicting daily variations in temperature and solar radiation in this paper are accurate. Furthermore, they exhibit high prediction accuracy even when only the daily maximum and minimum temperatures are provided.

This paper considered the characteristics of both accumulation and hysteresis in influencing the temperature and solar radiation on an asphalt surface. Thus, it employed a high-temperature asphalt pavement monitoring test to collect 1015 sets of data. Furthermore, Pearson correlation analysis was performed on the average temperature T_a and solar radiation intensity Q. it is provided by Equation (3).

$$R = \frac{1}{n-1}\sum_{i=1}^{n}\left(\frac{X_i - \bar{X}}{S_X}\right)\left(\frac{Y_i - \bar{Y}}{S_Y}\right) \tag{3}$$

In Equation (3), n denotes the number of samples, while X_i and Y_i represent the observed values of these samples. Furthermore, $\overline{X}$ and $\overline{Y}$ indicate the average value of the two samples, while S_X and S_Y denote the standard deviation of the sample. The correlation coefficient results are presented in TABLE III.

TABLE III. Fitted model parameters for the daily variation in air temperature and solar radiation intensity

INFLUENCE FACTOR	1H	2H	3H	4H	5H	6H	7H	8H	9H
AIR TEMPERATURE	0.957	0.932	0.892	0.803	0.517	0.425	0.285	0.128	0.037
SOLAR RADIATION INTENSITY	0.931	0.945	0.952	0.969	0.914	0.863	0.629	0.530	0.377

The surface temperature has the greatest correlation with the average solar radiation intensity in the previous four hours and the average air temperature in the previous hour. Therefore, a model for the pavement's surface temperature must account for these two parameters. Compared to air temperature and solar radiation, the daily variation in wind speed is extremely unstable and results in large errors between the prediction and fitting process. Thus, the current paper incorporated only the daily average wind speed into this model.

Combined with the above analysis, the parameters related to air temperature and solar radiation intensity may be determined. By incorporating the daily average wind speed, a prediction model for predicting surface temperature was established. The representation of the model is provided by Equation (4).

$$T(t) = A_1 T_a(t) + A_2 \overline{T}_{a1h}(t) + A_3 Q(t - 2.5h) + A_4 \overline{Q}_{4h}(t) + A_5 \overline{T}_a v \qquad (4)$$

Where $A_1 \sim A_6$ ——parameters to be fitted;
$\overline{T}_{a1h}$——average air temperature in previous 1 h;
$\overline{Q}_{4h}$——average solar radiation intensity in previous 4 h;
$\overline{T}_a$——average value of daily maximum and minimum air temperature;
v——daily average wind speed

After fitting the Equation (4) parameters and according to the daily temperature extreme value and the daily average wind speed, a 24-hour prediction for the surface layer temperature may be made. A comparison between the measured surface temperature and the predictions is illustrated in the following Fig 12, TABLE IV.
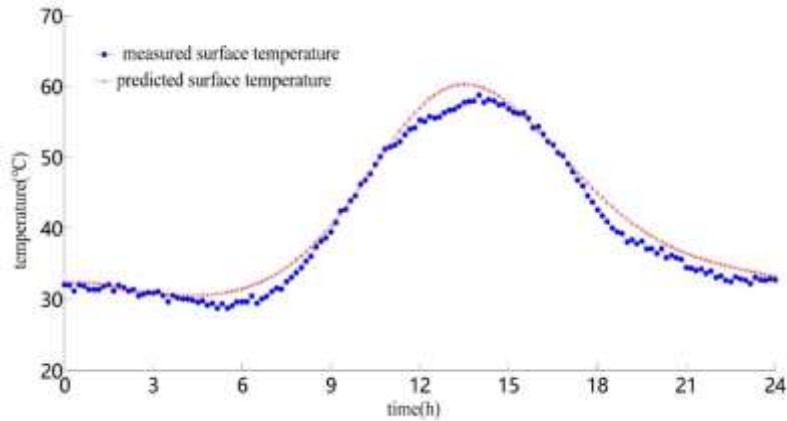
Fig 12: Comparison of measured and predicted surface temperatures on September 5th

TABLE IV. Deviations between measured and predicted surface temperatures on different dates (℃)

DATE	SEPTEMBER 5TH	SEPTEMBER 11TH	SEPTEMBER 12TH	SEPTEMBER 13TH
MAXIMUM DEVIATION	2.84	2.51	2.89	2.74
AVERAGE DEVIATION	1.25	1.34	1.31	1.27

Even if only the daily maximum temperature, minimum temperature, and average wind speed are provided, the prediction model represented by Equation 3.4 still has a high prediction accuracy for measuring the surface temperature of asphalt pavement. Since this data can be directly obtained from meteorological stations, the model has practical applicability as well. However, the parameters of Equation (4) need to be fitted and continuously updated based on short-term measured data. In practical applications, this model heavily relies on the accuracy of weather forecasts made by meteorological stations.

2.4 Theoretical Predictions for the Temperature Field in Asphalt Pavement

Asphalt pavement is typically composed of the surface layer and base layer. Therefore, a multi-layer flat structure model was constructed based on different pavement materials. To enhance the calculation accuracy of the temperature field, the thermal performance parameters at each position are closer to the actual situation. To obtain the temperature field in the double-layer asphalt pavement structure, this paper introduces a model consisting of the exact solution to Green's function.

(1) Initial assumptions

There are several relevant assumptions for the temperature field model for multi-layer asphalt pavement. Firstly, each structural layer is a uniform and continuous isotropic body. Secondly, the model

considers only temperature variation in relation to changes in depth the thermal performance parameters of pavement material and the lower boundary temperature of pavement structure are taken to be constant. Fourthly, the temperature field variation examines 24-hour cycles. Lastly, each structural layer of pavement is closely bonded. The temperature between the upper and lower contact surfaces is equal, while the heat flow is continuous.

(2) Mathematical model

A one-dimensional unsteady heat conduction Equation for multi-layer asphalt pavement was constructed. It is provided by Equation (5).

$$\alpha_i \frac{\partial^2 T_i(z,t)}{\partial z^2} = \frac{\partial T_i(z,t)}{\partial t} \quad H_{i-1} < z < H_i, t > 0 \tag{5}$$

In Equation (5), $i = 1,2,3,\dots,n$, while H_i denotes the depth of the lower boundary of the i-th layer away from the surface (m) and $H_0 = 0$.

Initial condition:

$$T_i(z,t) = F_i(z) \quad H_{i-1} < z < H_i, t = 0 \tag{6}$$

Boundary conditions:

$$T_1(z,t) = f_1(t) \quad z = 0, t > 0 \tag{7}$$

$$\left.\begin{array}{l} T_i(z,t) = T_{i+1}(z,t) \\ k_i \dfrac{\partial T_i}{\partial z} = k_{i+1} \dfrac{\partial T_i}{\partial z+1} \end{array}\right\} \quad z = H_i, i = 1,2,3,\dots,n-1, t > 0 \tag{8}$$

$$T_n(z,t) = f_n \quad z = H_n, t > 0 \tag{9}$$

Above, $f_1(t)$ denotes the variation in surface temperature with time, while f_2 represents a constant.

The above model adopted the surface temperature prediction model constructed as the first type of upper boundary condition in the heat conduction Equation. It further selected the unsteady temperature field in the double-layer asphalt pavement structure to obtain accurate results.

(3) Model calculation

According to previous research, the exact solution for the temperature field in double-layer asphalt pavement lacks an internal heat source and is expressed by Green's function as follows [10]:

$$T_i(z,t) = \alpha_1 \int_0^t \left(\left. \frac{\partial G_{i1}\left(z,t|z',\tau\right)}{\partial z'} \right|_{z'=H_0} f_1(\tau) \right) d\tau - \alpha_2 \int_0^t \left(\left. \frac{\partial G_{i2}\left(z,t|z',\tau\right)}{\partial z'} \right|_{z'=H_2} f_2(\tau) \right) d\tau$$

$$+ \sum_{j=1}^2 \int_{H_{j-1}}^{H_j} G_{ij}\left(z,t|z',\tau\right)\Big|_{\tau=0} F_j\left(z'\right) dz' \quad i = 1,2 \quad (10)$$

Green's function corresponding to the original problem is as follows:

$$G_{ij}\left(z,t|z',\tau\right) = \sum_{n=1}^\infty e^{-\beta_n^2(t-\tau)} \left(\sum_{j=1}^2 \frac{k_j}{\alpha_j} \int_{H_{j-1}}^{H_j} \chi_{jn}^2\left(z'\right) dz' \right)^{-1} \frac{k_j}{\alpha_j} \chi_{in}(z)\chi_{jn}\left(z'\right) \quad (11)$$

Equation (10) and Equation (11) constitute the exact solution for the temperature field in double-layer asphalt pavement. Each pavement layer corresponds to different expressions of the exact solution and Green's functions.

The constructed model was compiled into MATLAB language and calculated. During this process, the temperature field was substituted into the calculation as the singularity condition of the calculation model. Furthermore, in the above model, the thermal diffusivities were taken to be 0.810^{-6} m^2/s and 0.710^{-6} m^2/s in the surface layer and base layer, respectively. The thermal conductivities were taken to be 1.5 W/(m·K) and 1.2 W/(m·K). Moreover, the thermal diffusivity for single-layer pavement was weighted according to the thickness of the pavement's structure layer, which was measured as 0.73×10^{-6} m^2/s [20, 21]. The exact solution for the temperature field in the single-layer and double-layer pavement at the depth of 0.05 m and 0.15 m were compared with the measured values. The comparison is illustrated in Fig 13, Fig 14, TABLE V.
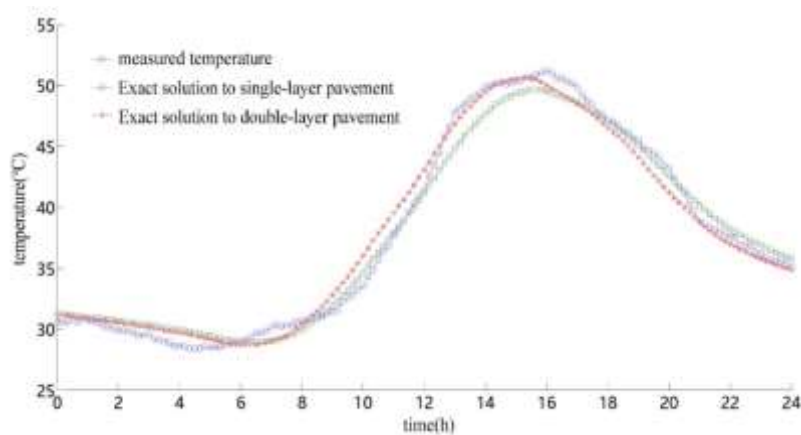

Fig 13: Comparison of measured and predicted temperature at a depth of 0.05 m on September 12th
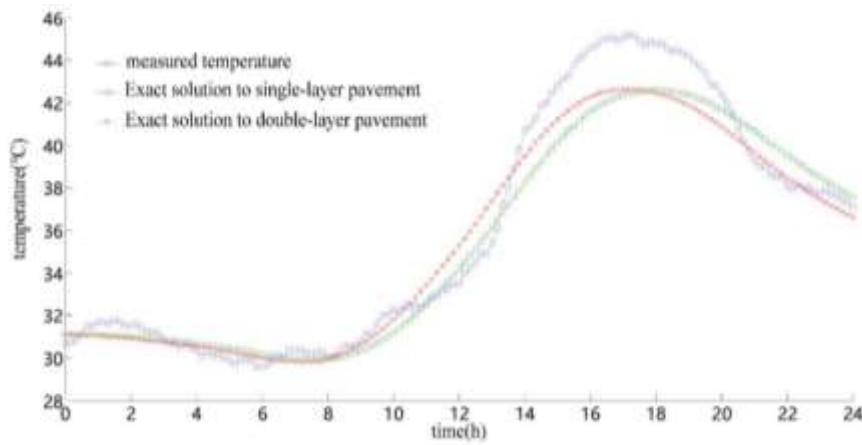
Fig 14: Comparison of temperature predictions and measured result at a depth of 0.15 m on September 12th

TABLE V. Average absolute deviation of temperature field predictions provided by different models (℃)

DATE	SEPTEMBER 11TH		SEPTEMBER 12TH		SEPTEMBER 13TH	
DEPTH (M)	0.05	0.15	0.05	0.15	0.05	0.15
SINGLE LAYER PAVEMENT MODEL	1.02	1.16	0.98	1.21	1.10	1.24
DOUBLE-LAYER PAVEMENT MODEL	1.13	1.19	1.06	1.19	1.14	1.17

For both single-layer and double-layer calculation models, the prediction results appeared to be relatively similar. For the three typical high-temperature days, the mean absolute deviations at a depth of 0.05 m predicted by single-layer and double-layer pavement model differed by 0.077 °C. Those at a depth of 0.15 m differ by 0.02 °C.

If there is an error in the upper boundary conditions of the prediction model and the measured temperature field, the predictions of single-layer and two-layer models are similar in practical prediction applications. This is due to the fact that the empirical thermal performance parameters of the surface layer and base layer do not differ significantly.

III. CONCLUSIONS

This paper combines statistical analysis and theoretical mathematical calculation to analyze relevant data and make theoretical predictions about the temperature field in high-temperature asphalt pavement. Several conclusions have been drawn and are presented below:

(1) Firstly, both the double sine and quasi-normal distribution function were employed to fit the daily variations in air temperature and solar radiation intensity. Furthermore, an empirical prediction model for determining the surface temperature of asphalt pavements was established based on several environmental factors. The maximum daily deviation between the predicted result and measured data amounted to 1.35 °C.

(2) To establish a model for predicting the pavement's unsteady temperature field, the asphalt pavement was simplified into a single-layer and double-layer plate structure. The actual predictions of the two models were compared based on the measured data. The results indicated that the pavement's temperature field obtained by the single-layer and double-layer models were similar overall. The maximum daily average deviation between the predicted results and the measured data was measured to be 1.24 ℃.

This research provides theoretical basis for the evaluation of long-term serving performance of asphalt pavement, as well as for pavement structure design and material improvement.

REFERENCES

[1] Higashiyama H, Sano M, Nakanishi F, et al. Field measurements of road surface temperature of several asphalt pavements with temperature rise reducing function. Case Studies in Construction Materials, 2016, 4:73-80.

[2] Aitbayev, Koblanbek, Teltayev, et al. Modeling of Transient Temperature Distribution in Multilayer Asphalt Pavement. Geomechanics & Engineering, 2015.

[3] Han R, Jin X, Glover C J. Modeling Pavement Temperature for Use in Binder Oxidation Models and Pavement Performance Prediction. Journal of Materials in Civil Engineering, 2011, 23(4):351-359.

[4] Abo-Hashema M A. Modeling Pavement Temperature Prediction Using Artificial Neural Networks. American Society of Civil Engineers, 2014:490-505.

[5] Mohammad Z, Alavi, et al. Prediction of Asphalt Pavement Temperature Profile with Finite Control Volume Method. Transportation Research Record, 2018, 2456(1):96-106.

[6] Ariawan I M A, Subagio B S, Setiadji B H. Development of Asphalt Pavement Temperature Profile Model for Tropical Climate Conditions in the Eastern Bali Region, Indonesia. 2015.

[7] Sreedhar S, Biligiri K P. Development of Pavement Temperature Predictive Models Using Thermophysical Properties to Assess Urban Climates in the Built Environment. Sustainable Cities & Society, 2016, 22:78-85.

[8] Chandrappa A K, Biligiri K P. Development of Pavement-Surface Temperature Predictive Models: Parametric Approach. Journal of Materials in Civil Engineering, 2016, 28(3):04015143.1-04015143.12.

[9] Al-Kalbani A, Farag S G. Pavement Temperature Prediction Model for Oman Climate Condition. Journal of Student Research, 2017.

[10] Chen J, Wang H, Zhu H. Analytical approach for evaluating temperature field of thermal modified asphalt pavement and urban heat island effect. Applied Thermal Engineering, 2017, 113:739-748.

[11] Yinfei D, Qin S, Shengyue W. Bidirectional heat induced structure of asphalt pavement for reducing pavement temperature. Applied Thermal Engineering, 2015, 75:298-306.

[12] Khan Z, Islam M R, Tarefder R A. Determining the average asphalt temperature of flexible pavement//4th Geo-China International Conference., 2016:113-119.

[13] Jia L, Sun L, Yu Y. Asphalt Pavement Statistical Temperature Prediction Models Developed from Measured Data in China// International Conference of Chinese Transportation Professionals Congress. 2008.

[14] Teltayev B, Aitbayev K. Modeling of transient temperature distribution in multilayer asphalt pavement. Geomechanics & engineering, 2015, 8(2):133-152.

[15] Islam M R, Ahsan S, Tarefder R A. Modeling Temperature Profile of Hot-Mix Asphalt in Flexible Pavement. International Journal of Pavement Research & Technology, 2015, 8(1):47-52.

[16] Qin Yinghong. Pavement Surface Maximum Temperature Increases Linearly with Solar Absorption and Reciprocal Thermal Inertial. International Journal of Heat & Mass Transfer, 2016, 97:391-399.

[17] Teltayev B, Aitbayev K. Modeling of temperature field in flexible pavement. Indian Geotechnical Journal, 2015, 45(4):371-377.

[18] Zhu D. Temperature field numerical analysis of asphalt pavement//2018 7th International Conference on Energy, Environment and Sustainable Development (ICEESD 2018). Atlantis Press, 2018:846-852.

[19] Li Y, Zhang Q, Xie L, et al. Testing of asphalt mixture thermal conductivity and its influences on asphalt pavement temperature field. Journal of Functional Materials, 2012: S1.

[20] Yan X, Chen L, You Q, et al. Experimental Analysis of Thermal Conductivity of Semi-Rigid Base Asphalt Pavement. Road Materials and Pavement Design, 2019, 20(5-6):1215-1227.

[21] Chadbourn B A, Newcomb D, Voller V, et al. An Asphalt Paving Tool for Adverse Conditions. Center for Transportation Studies, 1998.